ECMWF COPERNICUS REPORT

Copernicus Climate Change Service

Algorithm Theoretical Basis Document (ATBD) – ANNEX D for products XCO2_EMMA, XCH4_EMMA, XCO2_OBS4MIPS, XCH4_OBS4MIPS (v4.3, 01/2003-06/2020)

C3S_312b_Lot2_DLR – Atmosphere

Issued by: Maximilian Reuter, University of Bremen,

Institute of Environmental Physics (IUP)

Date: 18/02/2021

Ref: C3S_D312b_Lot2.1.3.2-v3.0_ATBD-GHG_ANNEX-D_v5.0

Official reference number service contract: 2018/C3S_312b_Lot2_DLR/SC1

IMPLEMENTED BY ECMWF

Contributors

INSTITUTE OF ENVIRONMENTAL PHYSICS (IUP), UNIVERSITY OF BREMEN, BREMEN, GERMANY

(IUP)

M. Reuter

M. Buchwitz

O. Schneising-Weigel

Table of Contents

History of modifications

Version	Date	Description of modification	Chapters / Sections
1.1	20-October-2017	New document for data set CDR1 (2003-2016)	All
2.0	4-October-2018	Update for CDR2 (2003-2017)	All
3.0	12-August-2019	Update for CDR3 (2003-2018)	All
3.1	03-November-2019	Update after review by Assimila: Correction of typos, text improvements, additional explanations added, figure captions moved to above figures.	All
4.0	18-August-2020	Update for CDR4 (2003-2019)	All
5.0	18-February-2021	Update for CDR5 (01/2003-06/2020)	All

Related documents

Reference ID	Document
D1	Main ATBD: **Buchwitz, M., et al.:** Algorithm Theoretical Basis Document (ATBD) – Main document for Greenhouse Gas (GHG: CO_2 & CH_4) data set CDR 5 (01.2003-06.2020), project C3S_312b_Lot2_DLR – Atmosphere, v5.0, 2021. *(this document is an ANNEX to the Main ATBD)*
D2	**Reuter et al.:** Product Quality Assessment Report (PQAR) – ANNEX D for products XCO2_EMMA, XCH4_EMMA, XCO2_OBS4MIPS, XCH4_OBS4MIPS, project C3S_312b_Lot2_DLR – Atmosphere, v5.0, 2021.

Acronyms

Acronym	Definition
AIRS	Atmospheric Infrared Sounder
AMSU	Advanced Microwave Sounding Unit
ATBD	Algorithm Theoretical Basis Document
BESD	Bremen optimal EStimation DOAS
CAR	Climate Assessment Report
C3S	Copernicus Climate Change Service
CCDAS	Carbon Cycle Data Assimilation System
CCI	Climate Change Initiative
CDR	Climate Data Record
CDS	(Copernicus) Climate Data Store
CMUG	Climate Modelling User Group (of ESA's CCI)
CRG	Climate Research Group
D/B	Data base
DOAS	Differential Optical Absorption Spectroscopy
EC	European Commission
ECMWF	European Centre for Medium Range Weather Forecasting
ECV	Essential Climate Variable
EMMA	Ensemble Median Algorithm
ENVISAT	Environmental Satellite (of ESA)
EO	Earth Observation
ESA	European Space Agency
EU	European Union
EUMETSAT	European Organisation for the Exploitation of Meteorological Satellites
FCDR	Fundamental Climate Data Record
FoM	Figure of Merit
FP	Full Physics retrieval method
FTIR	Fourier Transform InfraRed

FTS	Fourier Transform Spectrometer
GCOS	Global Climate Observing System
GEO	Group on Earth Observation
GEOSS	Global Earth Observation System of Systems
GHG	GreenHouse Gas
GOME	Global Ozone Monitoring Experiment
GMES	Global Monitoring for Environment and Security
GOSAT	Greenhouse Gases Observing Satellite
IASI	Infrared Atmospheric Sounding Interferometer
IMAP-DOAS (or IMAP)	Iterative Maximum A posteriori DOAS
IPCC	International Panel in Climate Change
IUP	Institute of Environmental Physics (IUP) of the University of Bremen, Germany
JAXA	Japan Aerospace Exploration Agency
JCGM	Joint Committee for Guides in Metrology
L1	Level 1
L2	Level 2
L3	Level 3
L4	Level 4
LMD	Laboratoire de Météorologie Dynamique
MACC	Monitoring Atmospheric Composition and Climate, EU GMES project
NA	Not applicable
NASA	National Aeronautics and Space Administration
NetCDF	Network Common Data Format
NDACC	Network for the Detection of Atmospheric Composition Change
NIES	National Institute for Environmental Studies
NIR	Near Infra Red
NLIS	LMD/CNRS *neuronal* network mid/upper tropospheric CO2 and CH4 retrieval algorithm
NOAA	National Oceanic and Atmospheric Administration
Obs4MIPs	Observations for Climate Model Intercomparisons

OCO	Orbiting Carbon Observatory
OE	Optimal Estimation
PBL	Planetary Boundary Layer
ppb	Parts per billion
ppm	Parts per million
PR	(light path) PRoxy retrieval method
PVIR	Product Validation and Intercomparison Report
QA	Quality Assurance
QC	Quality Control
REQ	Requirement
RMS	Root-Mean-Square
RTM	Radiative transfer model
SCIAMACHY	SCanning Imaging Absorption spectroMeter for Atmospheric ChartographY
SCIATRAN	SCIAMACHY radiative transfer model
SC2C	Simple CO_2 Climatological model
SC4C	Simple CH_4 Climatological model
SECM	Simple Empirical CO_2 Model
SRON	SRON Netherlands Institute for Space Research
SWIR	Short Wava Infra Red
TANSO	Thermal And Near infrared Sensor for carbon Observation
TANSO-FTS	Fourier Transform Spectrometer on GOSAT
TBC	To be confirmed
TBD	To be defined / to be determined
TCCON	Total Carbon Column Observing Network
TIR	Thermal Infra Red
TR	Target Requirements
TRD	Target Requirements Document
WFM-DOAS (or WFMD)	Weighting Function Modified DOAS
UoL	University of Leicester, United Kingdom
URD	User Requirements Document

WMO	World Meteorological Organization
Y2Y	Year-to-year (bias variability)

General definitions

Table 1 lists some general definitions relevant for this document.

Table 1: General definitions.

Item	Definition
XCO2	Column-averaged dry-air mixing ratios (mole fractions) of CO_2
XCH4	Column-averaged dry-air mixing ratios (mole fractions) of CH_4
L1	Level 1 satellite data product: geolocated radiance (spectra)
L2	Level 2 satellite-derived data product: Here: XCO_2 and XCH_4 information for each ground-pixel
L3	Level 3 satellite-derived data product: Here: Gridded XCO_2 and XCH_4 information, e.g., 5°x5°, monthly
L4	Level 4 satellite-derived data product: Here: Surface fluxes (emission and/or uptake) of CO_2 and CH_4

Scope of document

This document is an Algorithm Theoretical Basis Document (ATBD) for the Copernicus Climate Change Service (C3S, https://climate.copernicus.eu/) greenhouse gas (GHG) component as covered by project C3S_312b_Lot2.

Within this project satellite-derived atmospheric carbon dioxide (CO_2) and methane (CH_4) Essential Climate Variable (ECV) data products are generated and delivered to ECMWF for inclusion into the Copernicus Climate Data Store (CDS) from which users can access these data products and the corresponding documentation.

The satellite-derived GHG data products are:

- Column-averaged dry-air mixing ratios (mole fractions) of CO_2 and CH_4, denoted XCO_2 (in parts per million, ppm) and XCH_4 (in parts per billion, ppb), respectively.
- Mid/upper tropospheric mixing ratios of CO_2 (in ppm) and CH_4 (in ppb).

This document describes the algorithms to generate the C3S products XCO2_EMMA, XCH4_EMMA, XCO2_OBS4MIPS and XCH4_OBS4MIPS.

These products are merged multi-sensor XCO_2 and XCH_4 Level 2 and Level 3 products generated using algorithms developed at University of Bremen, Germany.

For an overview of these merged Level 2 data products XCO2_EMMA and XCH4_EMMA and of these merged Level 3 data products XCO2_OBS4MIPS and XCH4_OBS4MIPS see also *Reuter et al., 2020*.

Executive summary

This ATBD describes the algorithm theoretical basis for EMMA v4.3 CO_2 and EMMA v4.3 CH_4. Originally, the EMMA algorithm (v1.3) was described in detail using the example of CO_2 in the publication of *Reuter et al. (2013).* More recently, *Reuter et al. (2020)* described the latest EMMA CO_2 and CH_4 developments and data sets. These publications are the blueprint for this ATBD.

For a long time, climate modelers have used ensemble approaches to calculate the ensemble median and to estimate uncertainties of climate projections where no ground-truth is known. Following this idea, the ensemble median algorithm EMMA brings together level 2 data of several SCIAMACHY, GOSAT, and OCO-2 XCO_2 and XCH_4 retrieval products independently developed by NASA, NIES, SRON, University of Leicester, and the University of Bremen. EMMA determines in 10°x10° degree grid boxes monthly averages and selects the level 2 data of the median algorithm. Thresholds depending on potential information content prevent from over-weighting individual algorithms with a considerably larger amount of data.

The EMMA database consists of individual level 2 soundings retrieved by algorithms which can change from grid box to grid box and month to month. Therefore, it can be used in the same manner as any other XCO_2 or XCH_4 satellite retrieval, i.e., the EMMA database includes all information needed for inverse modeling (geo-location, time, XCO_2 or XCH_4, averaging kernels, etc.). Additionally, it includes the inter-algorithm spread which informs about potential regional or temporal systematic uncertainties.

Obs4MIPs (Observations for Model Inter-comparisons Project) is an activity to make observational products more accessible especially for climate model inter-comparisons. Based on EMMA's XCO_2 and XCH_4 L2 data bases, the XCO2_OBS4MIPS and XCH4_OBS4MIPS data products are generated by spatial (5°x5°) and temporal (monthly) gridding. The output is stored in the Obs4MIPs NCDF format, which is described on the Obs4MIPs website: https://www.earthsystemcog.org/projects/obs4mips.

1. Data product overview

Our current knowledge about the sources and sinks of atmospheric CO_2 and CH_4 is limited by the sparseness of highly accurate and precise measurements of these gases (e.g., *Stephens et al., 2007*). Due to their global coverage and sensitivity down to the surface, satellite based XCO_2 and XCH_4 (column-average dry-air mole fraction of atmospheric CO_2 and CH_4) retrievals in the near infrared are promising candidates to reduce existing uncertainties if accurate and precise enough (e.g., *Rayner and O'Brien, 2001*; *Houweling et al., 2004*; *Miller et al., 2007*; *Chevallier et al., 2007*).

At present, several independently developed XCO_2 and/or XCH_4 retrieval algorithms exist for SCIAMACHY (SCanning Imaging Absorption spectroMeter of Atmospheric CHartographY; *Burrows et al., 1995*; *Bovensmann et al., 1999*), GOSAT (Greenhouse gases Observing SATtellite; *Yokota et al., 2004*), and OCO-2 (Orbiting Carbon Observatory-2; Crisp et al., 2017); see **Table 2** and **Table 3** for those used for EMMA v4.3 CO2 and EMMA v4.3 CH4, respectively.

All retrieval teams find encouraging validation results when comparing with TCCON (total carbon column observing network, *Wunch et al., 2011*) ground based FTS (Fourier transform spectrometer) measurements (see references in the next section). This goes along with a good inter-algorithm agreement at TCCON sites and with the results of our unified validation study having station-to-station biases (i.e., the standard deviation of the biases at different sites) usually below 0.6ppm and 5.0ppb and single measurement precisions usually below 2.0ppm and 14ppb for XCO_2 and XCH_4, respectively (**Figure 1**, **Figure 2**, **Table 4**, **Table 5**).

However, the inter-algorithm agreement often reduces remote from validation sites due to differing large scale bias patterns (see **Sec. 3.1**). Such biases can be a critical issue for surface flux inversions and the user requirements are demanding; as an example, *Miller et al. (2007)* and *Chevallier et al. (2007)* found that regional biases of a few tenths of a ppm can already hamper surface flux inversions. This indicates that assessing an algorithm's quality should not be based on comparisons against current TCCON stations only. Obviously, large regions of the world possess more "complicated" retrieval conditions without the availability of ground truth measurements which could be used to judge the algorithms' performance.

Diverging model results are common to many scientific disciplines (e.g., *Araujo and New, 2007*; *Rötter et al., 2011*) and much attention and effort is devoted to this topic on the subject of weather and climate modeling. Here, the divergence of the model results arises not only from structural differences of the different models, but also from the nonlinearity of the model equations, leading to differing results of one single model when performing multiple realizations with slightly differing initial conditions (*Hagedorn et al., 2005*; *Tebaldi and Knutti, 2007*).

Especially in the case of weather forecasting or climate projections, where no ground truth is available for the verification of the forecasts and projections, it is impossible to identify the "best" model and the "perfect" initial conditions. For long-term climate projections, this problem is impaired by the unknown future greenhouse forcing.

Table 2: Main retrieval characteristics of EMMA v4.3 CO_2 input XCO_2 data products: algorithm name and version, satellite instrument, spectral bands, inversion technique (OE = optimal estimation, TP = Tikhonov–Phillips regularization, LS = least squares), consideration of scattering (FP = full physics, PR = light path proxy, xEP20 = x extinction profiles with 20 layers (two aerosol types, water and ice cloud), ISL = isotropic scattering layer, TAU = scattering optical depth, SLH = scattering layer height, ANG = Angstrom exponent, CWP = cloud water path, CTH = cloud top height, AOD = aerosol optical depth, APNC = aerosol particle number concentration, ASP = aerosol size parameter, AH = aerosol height), main cloud filter (MERIS = medium resolution imaging spectrometer, TANSO-FTS = main instrument of GOSAT, TANSO-CAI = cloud and aerosol imager of GOSAT, PMD = polarization measurement device of SCIAMACHY).

Algorithm	Sensor	Bands [µm]				Inversion	Scattering	Primary cloud filter	Empirical bias correction
		0.76	1.58	1.60	2.05				
BESD v02.01.02	SCIAMACHY	•	•			OE	FP (CWP, CTH, APS1)	MERIS	•
ACOS v9r	GOSAT	•		•	•	OE	FP (4EP20)	TANSO-FTS	•
FOCAL v1.0	GOSAT	•		•	•	OE	ISL (TAU, SLH, ANG)	TANSO-FTS	•
RemoTeC v2.3.8	GOSAT	•		•	•	TP	FP (APNC, ASP, AH)	TANSO-CAI	•
UoL-FP v7.3	GOSAT	•		•	•	OE	FP (3EP20)	TANSO-FTS	•
NIES v02.9xbc	GOSAT	•		•	•	OE	FP (AOD)	TANSO-CAI	•
PPDF-s v02.xx	GOSAT	•		•	•	OE	PPDF parameters	TANSO-CAI	
NASA v10.2	OCO-2	•		•	•	OE	FP (4EP20)	OCO-2	•
FOCAL v09	OCO-2	•		•	•	OE	ISL (TAU, SLH, ANG)	MODIS	•

Table 3: Same as **Table 2** but for EMMA v4.3 CH_4 input XCH_4 data products.

Algorithm	Sensor	Bands [µm]				Inversion	Scattering	Primary cloud filter	Empirical bias correction
		0.76	1.58	1.60	2.05				
WFMD v4.0	SCIAMACHY	•	•			LS	PR (CH4/CO2)	PMD	•
RemoTeC-FP v2.3.8	GOSAT	•		•	•	TP	FP (APNC, ASP, AH)	TANSO-CAI	•
RemoTeC-PR v2.3.9	GOSAT	•		•	•	TP	PR (CH4/CO2)	TANSO-CAI	•
UoL-FP v7.3	GOSAT	•		•	•	OE	FP (3EP20)	TANSO-FTS	•
UoL-PR v9.0	GOSAT	•		•	•	OE	PR (CH4/CO2)	TANSO-FTS	•
NIES v02.9xbc	GOSAT	•		•	•	OE	FP (AOD)	TANSO-CAI	•
PPDF-S v02.xx	GOSAT	•		•	•	OE	FP (AOD)	TANSO-CAI	

Table 4: XCO_2 TCCON validation statistics for the period and sites shown in **Figure 1** with number of co-locations (#), average single measurement precision (σ) relative to TCCON and reported in brackets, and standard deviation of station-to-station biases (Δ).

Algorithm	#	σ [ppm]	Δ [ppm]
SCIAMACHY BESD v02.01.02	18611	1.79 (1.93)	0.27
GOSAT ACOS v9r	19707	1.65 (1.26)	0.33
GOSAT FOCAL v1.0	15412	1.90 (1.85)	0.36
GOSAT RemoTeC v2.3.8	14707	2.09 (2.18)	0.56
GOSAT UoL-FP v7.3	14680	1.80 (1.93)	0.38
GOSAT NIES v02.9xbc	18359	2.09 (0.98)	0.41
GOSAT PPDF-S v02.xx	8478	1.89 (0.76)	0.84
OCO-2 NASA v10.2	1823829	1.27 (0.53)	0.34
OCO-2 FOCAL v09	396111	1.45 (1.24)	0.25
EMMA v4.3 CO2	34623	1.59 (1.59)	0.35

Table 5: Same as **Table 4** but for XCH_4.

Algorithm	#	σ [ppm]	Δ [ppm]
WFMD v4.0	13258	99.30 (88.44)	8.25
RemoTeC-FP v2.3.8	13280	13.51 (13.62)	3.47
RemoTeC-PR v2.3.9	42803	13.85 (12.74)	2.29
UoL-FP v7.3	13242	12.90 (14.45)	2.74
UoL-PR v9.0	39602	13.35 (10.97)	4.48
NIES v02.9xbc	17103	12.91 (7.03)	3.74
PPDF-S v02.xx	7523	13.59 (5.11)	6.47
EMMA v4.3 CH4	24794	13.42 (13.53)	3.17

This conceptual problem is dealt with by using multi-model, multi-realization, multi-emission-scenario ensembles of simulations, which ideally span the entire range of possible model outcomes and, thus, can be used to estimate the uncertainties of the forecast or projection.

However, interpreting the ensemble's spread as uncertainty is not the only possible application: some studies indicate that the ensemble mean, weighted mean, or median can outperform each individual model under appropriate conditions (e.g., *Kharin and Zwiers, 2002*; *Vautard et al., 2009*).

Here, we seize this idea and introduce the ensemble median algorithm EMMA which uses data from the retrieval algorithms listed in **Table 2** and **Table 3** and within the next section. EMMA generates a database of individual level 2 retrievals and takes advantage of the variety of different retrieval algorithms and their independent developments.

For each month and each 10°×10° grid box, one algorithm is chosen to supply level 2 retrievals for the database. The algorithm is chosen on the basis that its grid box mean is the median amongst the available algorithms. This allows the reduction of occasional outliers and sometimes unrealistic bias patterns, which may be found in each individual retrieval algorithm and which may hamper surface flux inversions. EMMA relies on the assumption that it is unlikely that the majority of algorithms produce outliers in the same direction because only in this case the median is a bad choice.

Smoothing of real atmospheric variability, as it could happen when dealing with climate model ensembles, cannot be expected for EMMA because all ensemble members (XCO_2 or XCH_4 retrieval algorithms) represent the same (real) atmospheric XCO_2 or XCH_4 conditions and deviations from the real values are always due to retrieval errors (sampling issues are neglected in this context).

The EMMA database includes all information needed for inverse modeling (geo-location, time, XCO_2 or XCH_4, averaging kernels, etc.). As it consists of individual XCO_2 or XCH_4 retrievals, it can be used in the same manner as any other XCO_2 or XCH_4 satellite retrieval. Additionally, the EMMA database

includes the inter-algorithm spread which gives important information about regional and/or temporal systematic uncertainties.

Figure 1: Validation of individual XCO_2 algorithms and EMMA v4.3 CO_2 with TCCON GGG2014.

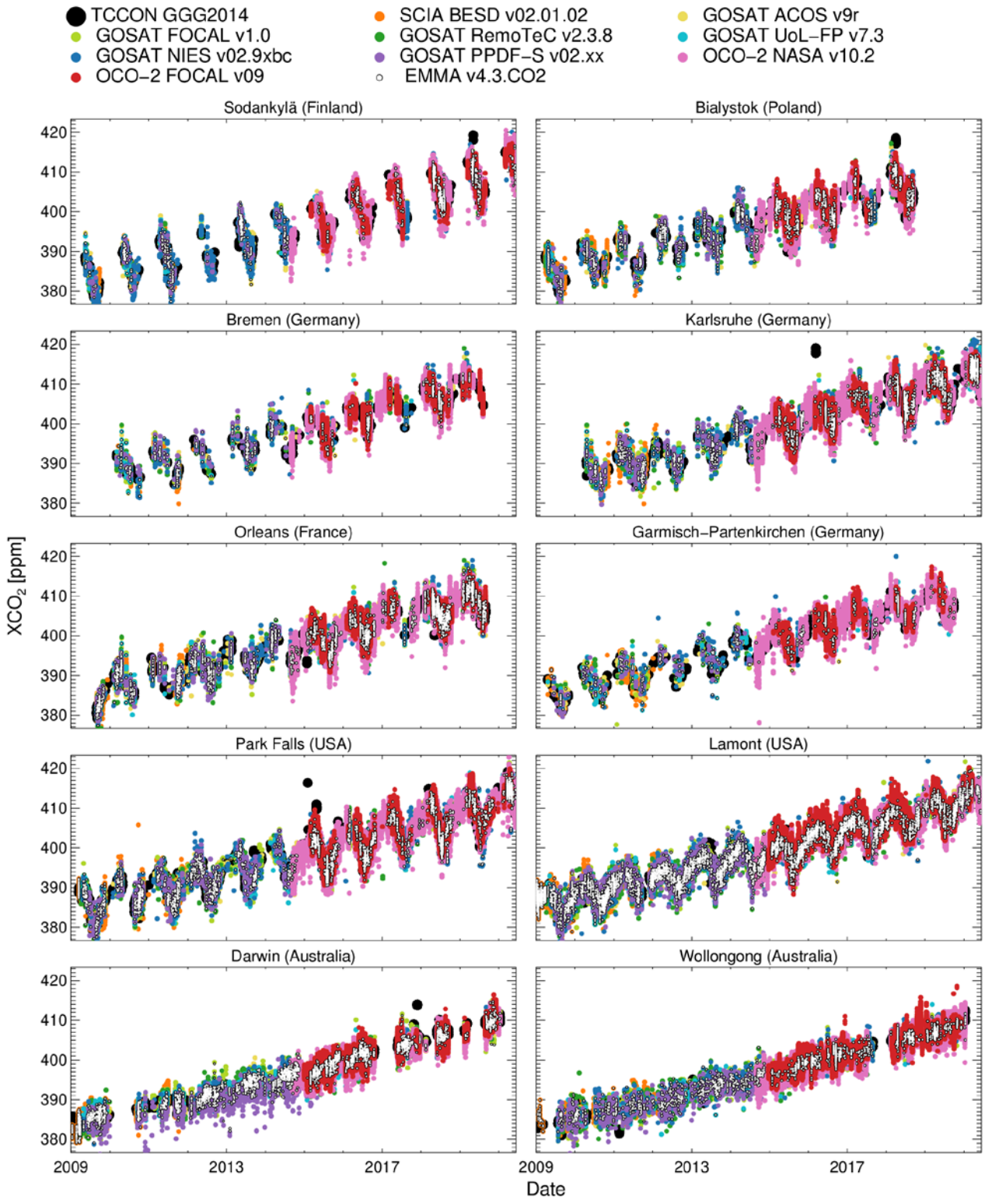

Figure 2: Validation of individual XCH_4 algorithms and EMMA v4.3 CH_4 with TCCON GGG2014.

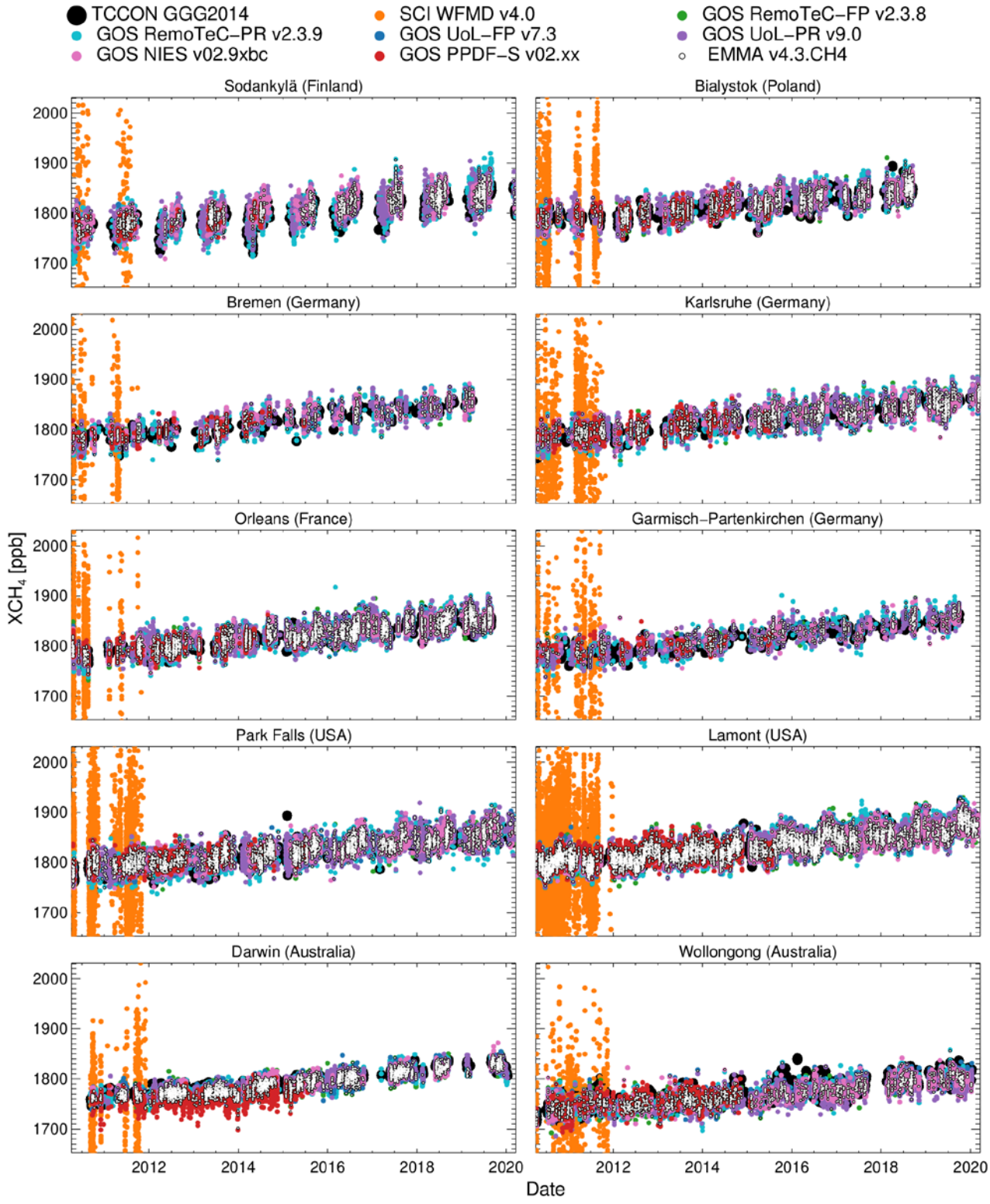

2. Input and auxiliary data

2.1. Satellite instrument

At present, several different XCO_2 and/or XCH_4 retrieval algorithms exist for SCIAMACHY, GOSAT, and OCO-2 which are under active development in order to meet the demanding user requirements, making them useful for surface flux inversions. Specifically, we make use of SCIAMACHY BESD v02.01.02 (*Reuter et al., 2016*), GOSAT FOCAL v1.0 (*Noël et al., 2020*), GOSAT ACOS v9r (*O'Dell et al., 2012*), GOSAT RemoTeC v2.3.8 (*Detmers et al., 2017a*), GOSAT UoL-FP v7.3 (*Boesch and Anand, 2017*), GOSAT NIES v02.9xbc (*Yoshida et al., 2013*), GOSAT NIES PPDF-S v02.xx (*Bril et al., 2012*), OCO-2 NASA v10.2 (*Kiel et al., 2019*), and OCO-2 FOCAL v09 (*Reuter et al., 2017a,b*) for XCO_2 and WFMD v4.0 (*Schneising et al., 2016*), RemoTeC-FP v2.3.8 (*Detmers et al., 2017a*), RemoTeC-PR v2.3.9 (*Detmers et al., 2017b*), UoL-FP v7.3 (*Boesch and Anand, 2017*), UoL-PR v9.0 (*Boesch and Anand, 2017*), NIES v02.9xbc (*Yoshida et al., 2011*), and PPDF-S v02.xx (*Bril et al., 2012*) for XCH_4.

The basic principle of all these algorithms is the same: (i) A satellite instrument measures backscattered solar radiation in near-infrared O_2 and CO_2 or CH_4 absorption bands. (ii) A radiative transfer plus instrument model (forward model) is utilized to simulate the satellite measurement for a set of known parameters (parameter vector) and unknown parameters (state vector). (iii) An inversion method tries to find that state vector which results in best agreement of simulated and measured radiances. (iv) The retrieved state vector is assumed to represent the true (or most likely) atmospheric state.

However, when going into more detail, the algorithms have distinct conceptual differences: the algorithms are optimized for different instruments (SCIAMACHY, GOSAT, or OCO-2). They are based on different absorption bands, use different inversion methods (optimal estimation, Tikhonov-Phillips, least squares), and are based on different physical assumptions on the radiative transfer in scattering atmospheres. In order to give two examples, so-called full physics algorithms explicitly account for (multiple) scattering at molecules, aerosols, and/or clouds by having state vector elements such as cloud water path, cloud top height, and aerosol optical thickness; the light path proxy method assumes that photon path lengths are modified similarly in the CO_2 and O_2 or CH_4 absorption bands, and that scattering related effects cancel out when dividing the retrieved CO_2 and O_2 or CH_4 columns when building XCO_2 or XCH_4. Additionally, the algorithms use different pre- and post-processing filters (e.g., cloud detection from O_2-A band or from a cloud and aerosol imager).

The main properties of the used retrieval algorithms are summarized in **Table 2** and **Table 3**. This list does not claim to be exhaustive and there are other aspects which can also easily result in differences of some ppm (e.g., spectroscopy). Discussions of the specific strengths and weaknesses and many more points, where the individual algorithms differ, can be found in the cited literature.

2.2. Other

In order to account for different column averaging kernels, all retrieval results are adjusted to a common a priori, namely the latest updates (2020) of the Simple CO_2 Climatological model (SC2C) or the Simple CH_4 Climatological model (SC4C). Both use a model-based climatology to estimate the spatial distribution and annual cycle of CO_2 or CH_4 which is adjusted for the annual growth.

SC4C has been developed by O.Schneising and briefly described by *Reuter et al., 2020*. In addition to its use as common a priori, SC4C has also been used as climatological training and calibration data set as described by *Schneising et al., 2019*.

The functioning of SC2C is very similar to that of SC4C. It is the successor of the Simple Empirical CO_2 Model (SECM, *Reuter et al., 2012)* and as for SECM, its climatological data base has been computed from mole fraction data of the recent version of NOAA's assimilation system CarbonTracker CT2019 (*Jacobson et al., 2020*).

Scaling the reported uncertainties and validation is done with TCCON (total carbon column observing network, *Wunch et al., 2011*) GGG2014 as reference data set.

3. Algorithms

3.1. EMMA ensemble spread

Due to entirely different samplings (different satellites, different filtering strategies, etc.), any algorithm inter-comparison considering the majority of individual soundings (level 2) can only be based on aggregated data (level 3), in our case monthly averages on a 10°×10° grid.

Before gridding, we apply the individual averaging kernels to adjust all retrieval results to a common a priori, namely the latest updates (2020) of the Simple CO_2 Climatological model (SC2C) or the Simple CH_4 Climatological model (SC4C) (see Sect. 2.2). We do this as proposed in the textbook of *Rodgers (2000)* and applied to XCO_2 by, for example, *Reuter et al. (2011)*. SC2C and SC4C reproduce large-scale features such as the year-to-year increase, the north/south gradient, and the seasonal cycle. However, SC2C and SC4C are only empirically extrapolating from past/averaged modeled CO_2 and CH_4 fields. New or changing phenomena cannot be within SC2C or SC4C, and it should also be mentioned that the adjustments are mostly minor, especially for CO_2 with typically a few tenths of a ppm.

For consistency, we remove the overall global bias of each retrieval with SC2C or SC4C as reference. In order to get statistically robust results, we only use those grid boxes with more than five soundings and for which the standard error of the mean is estimated to be less than 1ppm and 12ppb for XCO_2 and XCH_4, respectively. This takes the individual retrieval precisions into account so that the minimum number of soundings needed to build the average of a grid box can vary from retrieval to retrieval and grid box to grid box. Additionally, only grid boxes with a maximum number of overlapping algorithms (see **Figure 3**) are considered for the global bias adjustment. Beforehand, the reported retrieval precision is scaled to match (on average) the precision given in **Table 4** and **Table 5** obtained from a unified validation with TCCON data (**Figure 1** and **Figure 2**). **Figure 4** shows the influence of the global bias correction.

Figure 3: EMMA v4.3 input data availability (colored bars) and minimum number of used algorithms (gray) for median calculation for CO_2 (**left**) and CH_4 (**right**).

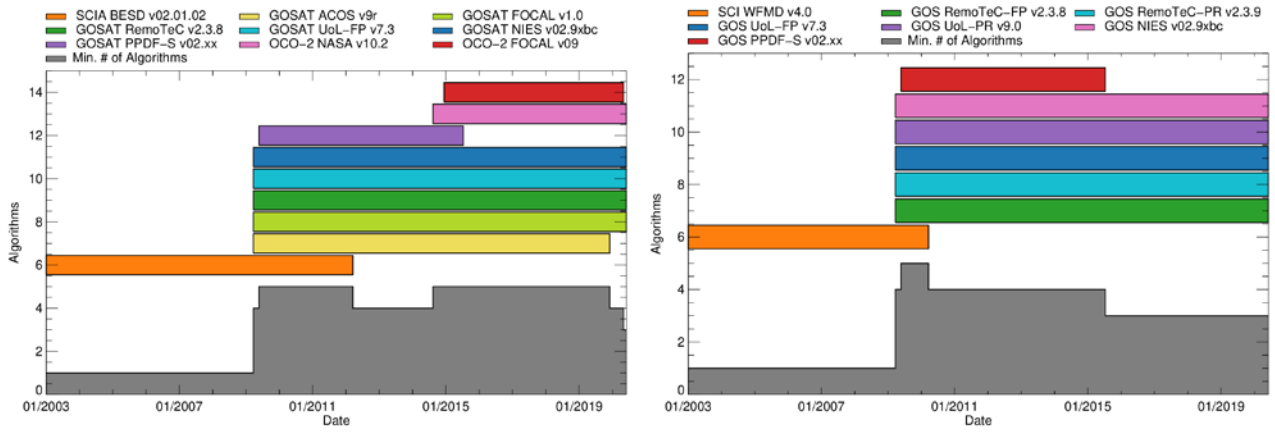

Figure 4: Global monthly average bias for XCO_2 (**left**) and XCH_4 (**right**) in common grid boxes relative to SC2C (XCO_2) and SC4C (XCH_4) before (**top**) and after (**bottom**) global bias correction.

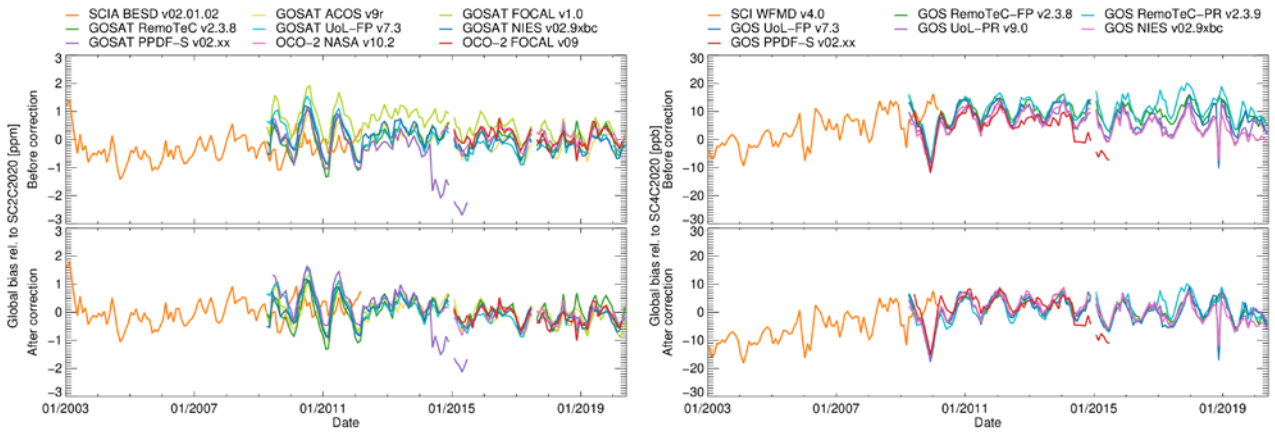

Figure 5 and **Figure 6** show at the example of April 2015 the calculated monthly XCO_2 or XCH_4 averages, respectively. First of all, one can see many large scale similarities such as the north/south gradient. However, one can also find more or less obvious outliers in the order of a percent for several algorithms. Often the observed systematic deviations (of level 3 data) are larger than expected from instrumental noise, i.e., they are dominated by specific algorithm effects. As level 3 grid boxes are always calculated from several individual level 2 soundings (ideally) sampled all over the grid box, we expect that sampling and representation errors are lower than the observed deviations. Therefore, these errors are not discussed further in this context.

Due to independent algorithm developments, different physical approaches and assumptions, different pre- and post-processing filters, and due to the different instruments, we expect relatively independent bias patterns. This is supported by **Figure 5** and **Figure 6**, which show (uncorrelated)

obvious outliers in various regions, i.e., it seems unlikely that all algorithms produce the same bias within one grid box. This implies that similar averages within one grid box can give us more confidence in the individual retrievals within this grid box. On the other hand, large inter-algorithm spreads indicate regions with more difficult and uncertain retrieval conditions. Therefore, we interpret the ensemble spread, i.e., the standard deviation, as uncertainty due to regional retrieval biases. An example is given in **Figure 7** showing larger inter-algorithm spreads for XCO_2 and XCH_4 in the tropics and in East Asia (mostly remote from TCCON sites). This pattern is temporally more or less stable, i.e., similar also in other months.

Figure 5: Monthly gridded XCO_2 averages and inter-algorithm spread at the example of April 2015 for EMMA v4.3 CO_2.

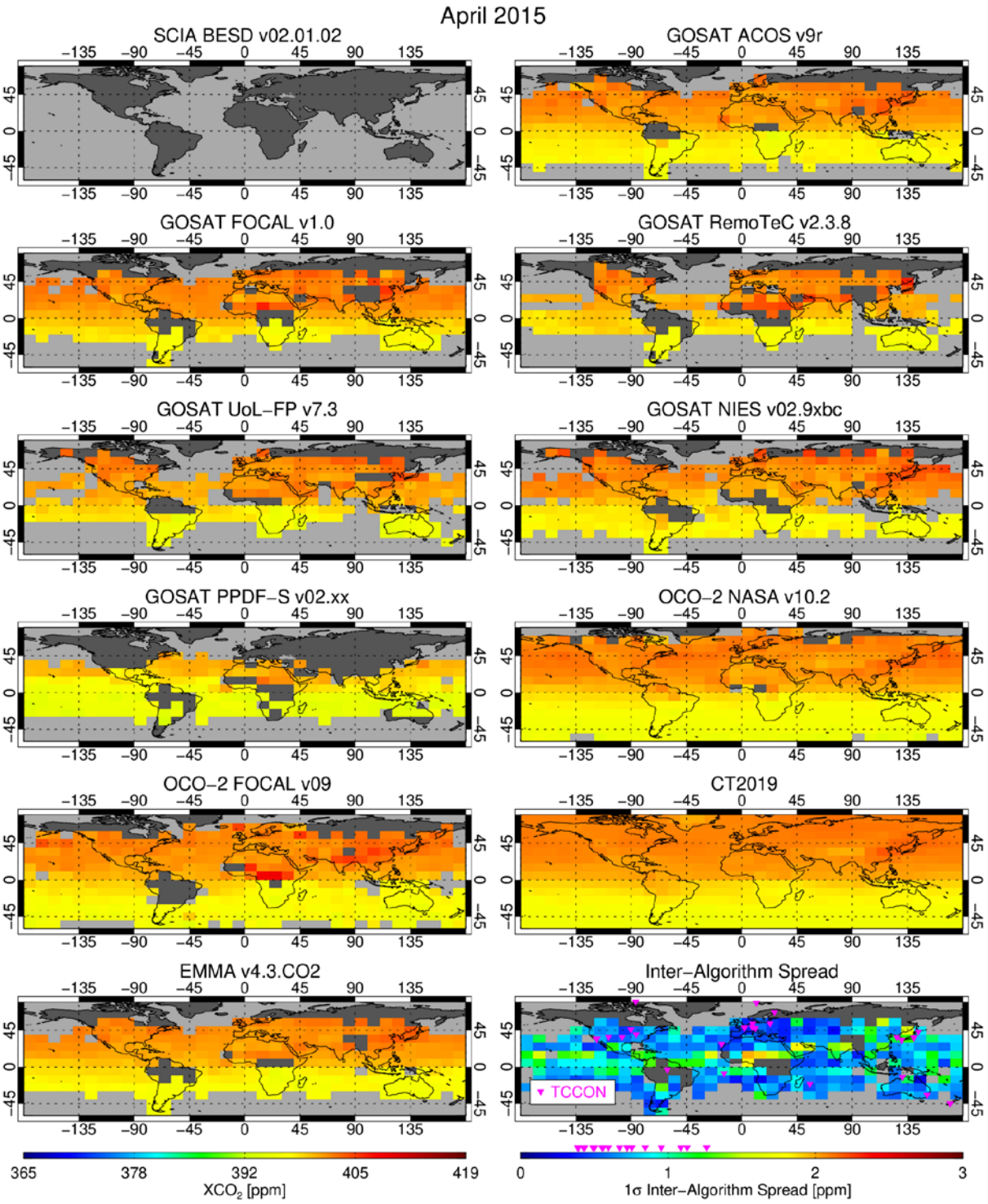

Figure 6: Monthly gridded XCH_4 averages and inter-algorithm spread at the example of April 2015 for EMMA v4.3 CH_4.

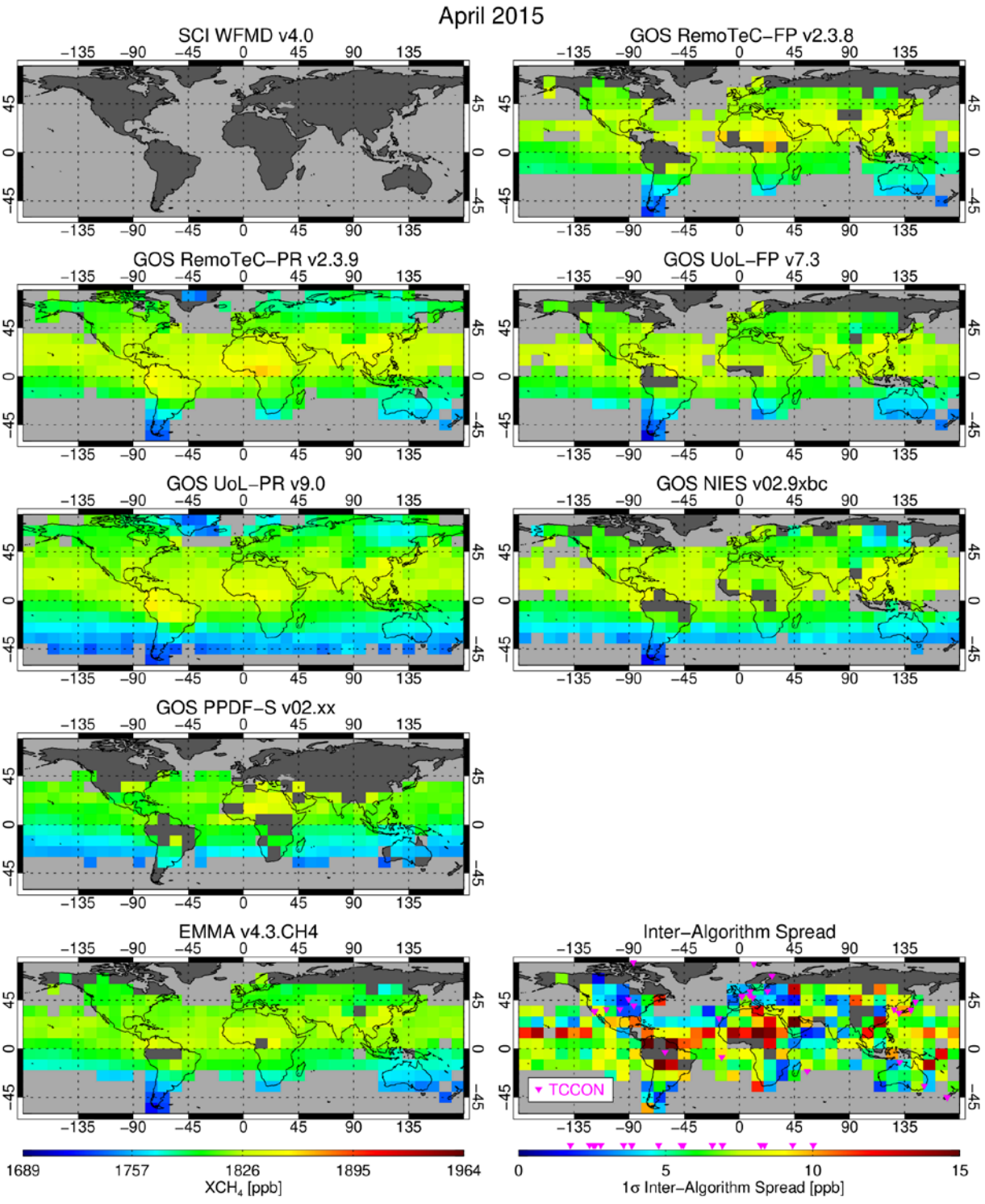

Figure 7: Average inter-algorithm spread (01/2003 – 06/2020) (**left**) and expected average inter-algorithm spread due to measurement noise (**right**) for EMMA v4.3 CO_2 (**top**) and EMMA v4.3 CH_4 (**bottom**).

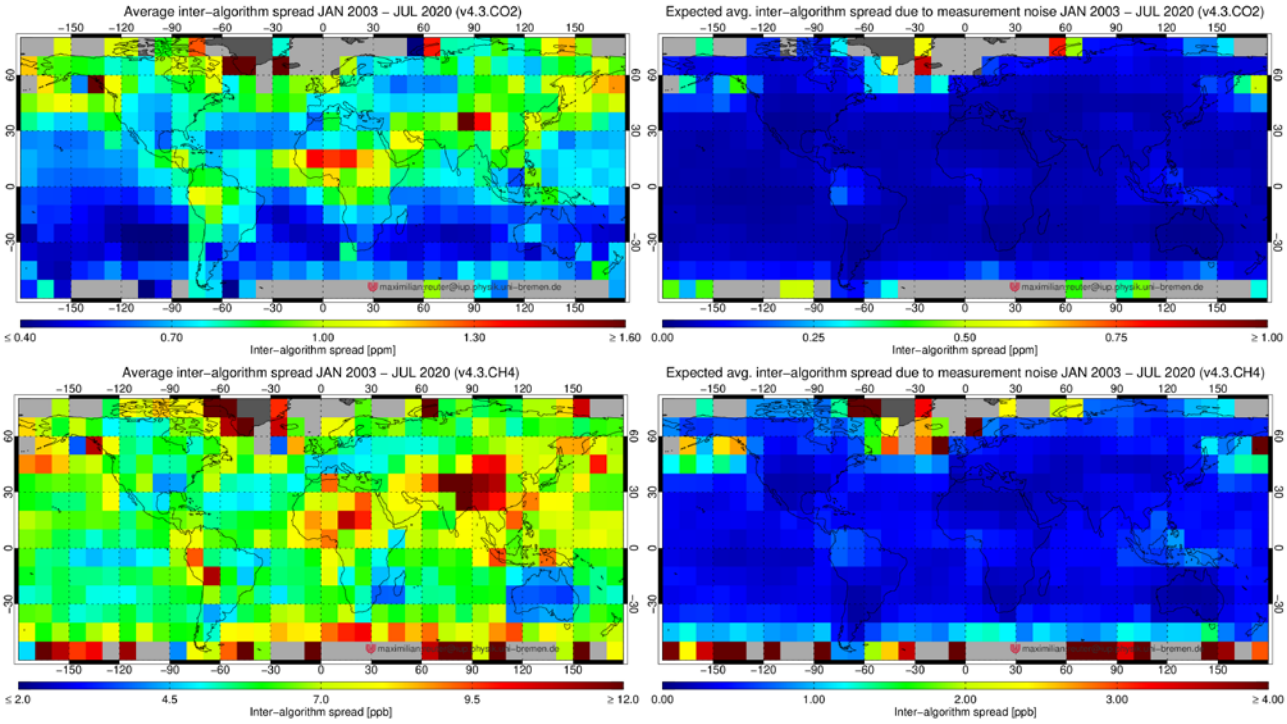

3.2. EMMA ensemble median

As described in the previous section, XCO_2 or XCH_4 averages (one for each algorithm) are calculated within each grid box. However, now, we are aiming to use the ensemble not only to assess regional and temporal uncertainties but also to create a data set which is potentially less influenced by regional or temporal biases. This could be achieved, for example, by building the average, a weighted average, or the median in each grid box.

In this context, the median has some advantages: outliers are assumed to be seldom and there is a high chance that a grid box includes no or only one outlying algorithm. Therefore, cancellation of errors cannot be expected by calculating the average. The median is much less sensitive to such individual outliers. Additionally, the median calculates no new quantity from the individuals of an ensemble, it is rather a procedure to select one specific ensemble member.

This allows us to trace back from level 3 averages to individual level 2 soundings. Essentially, there are five possible scenarios for median calculation within one grid box: (i) All algorithms perform well and scatter slightly around the true XCO2 or XCH4 value. In this case the median will help to reduce scatter. (ii) The minority of algorithms produce outliers so that the median is influenced only marginally. (iii) The majority of algorithms produce outliers in different directions. Here, it is still likely that the median falls on a well performing algorithm in the “middle”. (iv) The majority of algorithms produce outliers in the same direction. This is the only case where the median is a bad

choice, because it would select an outlier and ignore a well performing algorithm. As discussed in the previous section, we assume that the algorithms within one grid box are often realistic with uncorrelated occasional outliers, which makes this case unlikely to happen often. (v) If all algorithms are outlying, the median is not better or worse than selecting any other ensemble member.

We calculate the median only in grid boxes where reliable average XCO_2 or XCH_4 values can be computed for at least as many algorithms as specified in **Figure 3** (gray area). In case of an even number of values, we define the median as that value being closer to the mean. We then trace back to the individual level 2 data, which were used to calculate that average being the median. Together, with all information needed for inverse modeling (geo-location, time, averaging kernels, etc.), these soundings are stored in the EMMA database.

Some algorithms may provide considerably larger amounts of level 2 data (e.g., the NASA or FOCAL OCO-2 algorithm) than other algorithms. In order to prevent over-weighting these algorithms, we limit the maximum number of data points (per grid box). Therefore, we calculate the standard error of the mean of each successfully determined average. The idea behind this is that the lower the standard error of the mean, the larger the potential constraint on an inverse model becomes. If the standard error of the mean of the selected algorithm in a grid box is lower than $1/\sqrt{2}$ times the 25% percentile of all algorithms, the data points are randomly thinned accordingly. In this way, the number of data points can still be rather different but the potential constraint on an inverse model becomes similar.

3.3. OBS4MIPS

The L3 data products XCO2_OBS4MIPS and XCH4_OBS4MIPS are generated by spatial (5°x5°) and temporal (monthly) gridding of the corresponding EMMA L2 data bases. The gridding bases on arithmetic unweighted averaging of all soundings falling in a grid box. For each grid box, we compute the standard error of the mean by

$$\bar{\sigma} = \frac{1}{n}\sqrt{\sum \sigma_i}$$

where n is the number of soundings within the grid box and σ_i the (corrected) reported stochastic uncertainties of the soundings. In order to reduce noise within the level 3 product, we filter out grid boxes with $n \leq 1$ and $\bar{\sigma} > 1.6$ppm for XCO_2 or $\bar{\sigma} > 12$ppb for XCH_4, respectively.

Beside XCO_2 or XCH_4, the final level 3 product also includes the number of soundings used for averaging, the average column averaging kernel, the average a priori profile, the standard deviation of the averaged XCO_2 or XCH_4 values, and an estimate for the total uncertainty

$$\hat{\sigma} = \sqrt{\bar{\sigma}^2 + \sigma_s^2}.$$

Here, σ_s represents the inter-algorithm spread computed by EMMA averaged over the soundings within a grid box. For cases including only one algorithm, σ_s is replaced by quadratically adding spatial and seasonal accuracy determined from the TCCON validation (see D2, Table 2).

However, this is only the case during the SCIAMCHY-only period at the beginning of the time series (see **Figure 3**).

4. Output data

4.1. EMMA products

The EMMA database consists of individual level 2 soundings retrieved by algorithms which can change from grid box to grid box and month to month. Therefore, it can be used in the same manner as any other XCO_2 or XCH_4 satellite retrieval. **Figure 8** shows the relative data weight of each algorithm (defined as $\sum 1/\sigma_i^2$ normalized to one) within the EMMA database per month. The EMMA database includes all information needed for inverse modeling (geo-location, time, XCO_2 or XCH_4, averaging kernels, etc.). Additionally, it includes the inter-algorithm spread which informs about potential regional uncertainties.

At the example of April 2015, **Figure 9** shows the EMMA v4.3 XCO_2 or XCH_4 values as well as the corresponding selected median algorithm.

Note that the format of the main output data, which are the Level 2 data products, is described in the separate Product User Guide and Specification (PUGS) document.

Figure 8: EMMA v4.3 normalized relative data weight proportional to $\sum 1/\sigma_i^2$ (**top**) and number of soundings (**bottom**) per algorithm and month for CO_2 (**left**) and CH_4 (**right**).

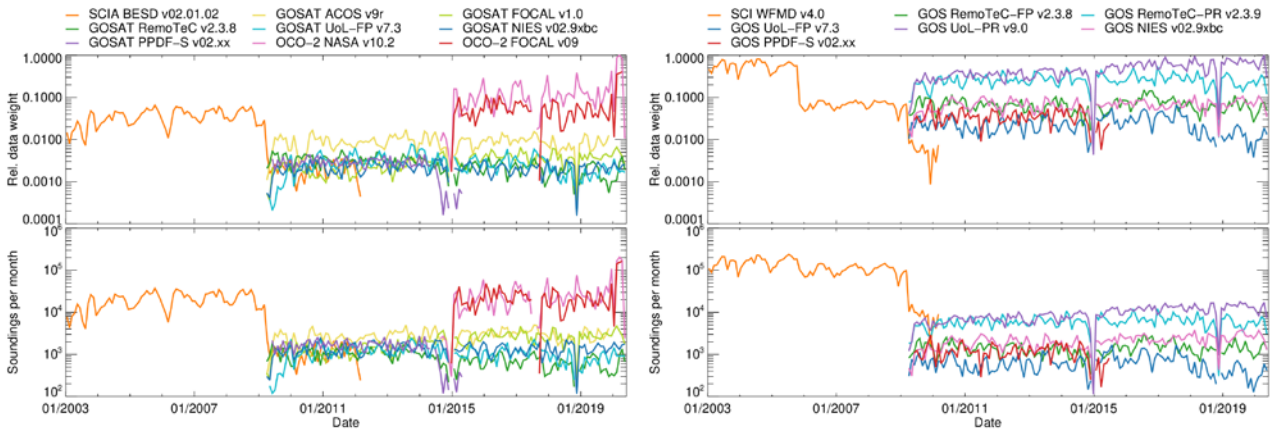

Figure 9: EMMA L2 XCO_2 and XCH_4 (**left**) and corresponding selected algorithm (**right**) for EMMA v4.3 CO_2 at the example of April 2015 (**top**) and EMMA v4.3 CH_4 at the example of Aril 2015 (**bottom**).

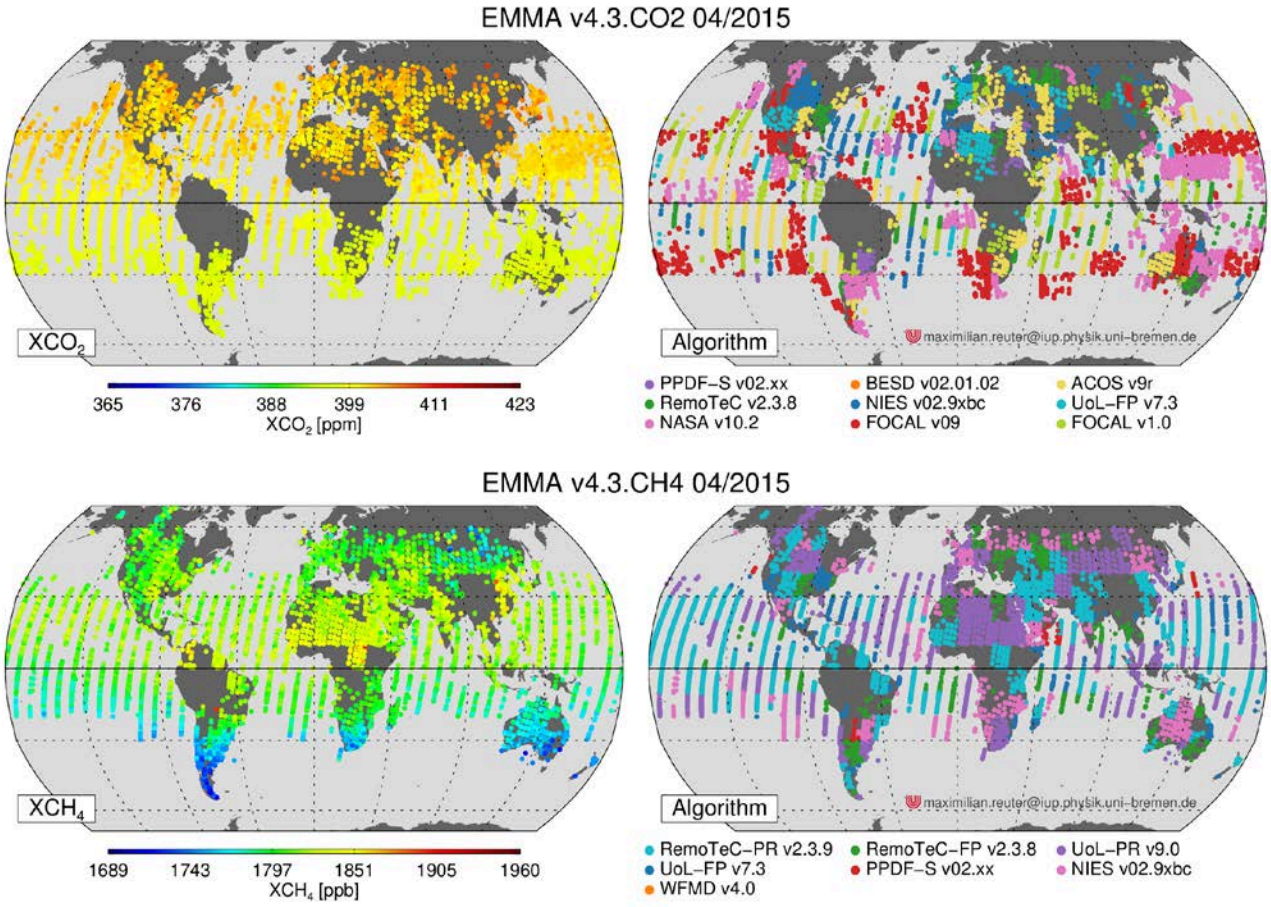

4.2. OBS4MIPS products

The XCO2_OBS4MIPS and XCH4_OBS4MIPS products consist of monthly, 5°x5° gridded level 3 XCO_2 or XCH_4 data computed from the corresponding EMMA databases. Additionally, the output files include gridded information about the number of averaged soundings, column averaging kernels, a priori profiles, standard deviation of XCO_2 or XCH_4, and an estimate of the total uncertainty accounting for measurement noise plus potential spatial and/or temporal biases.

At the example of April 2015, **Figure 10** shows the OBS4MIPS XCO_2 or OBS4MIPS XCH_4 values as well as the corresponding total uncertainty.

Note that the format of the output data, which are the level 3 data products, is described in the separate Product User Guide and Specification (PUGS) document (D2).

Figure 10: Top: XCO2_OBS4MIPS XCO2 for April 2015 (**left**) and its uncertainty computed from the retrieval noise and EMMA's inter-algorithm spread (**right**). Bottom: Same for XCH4_OBS4MIPS.

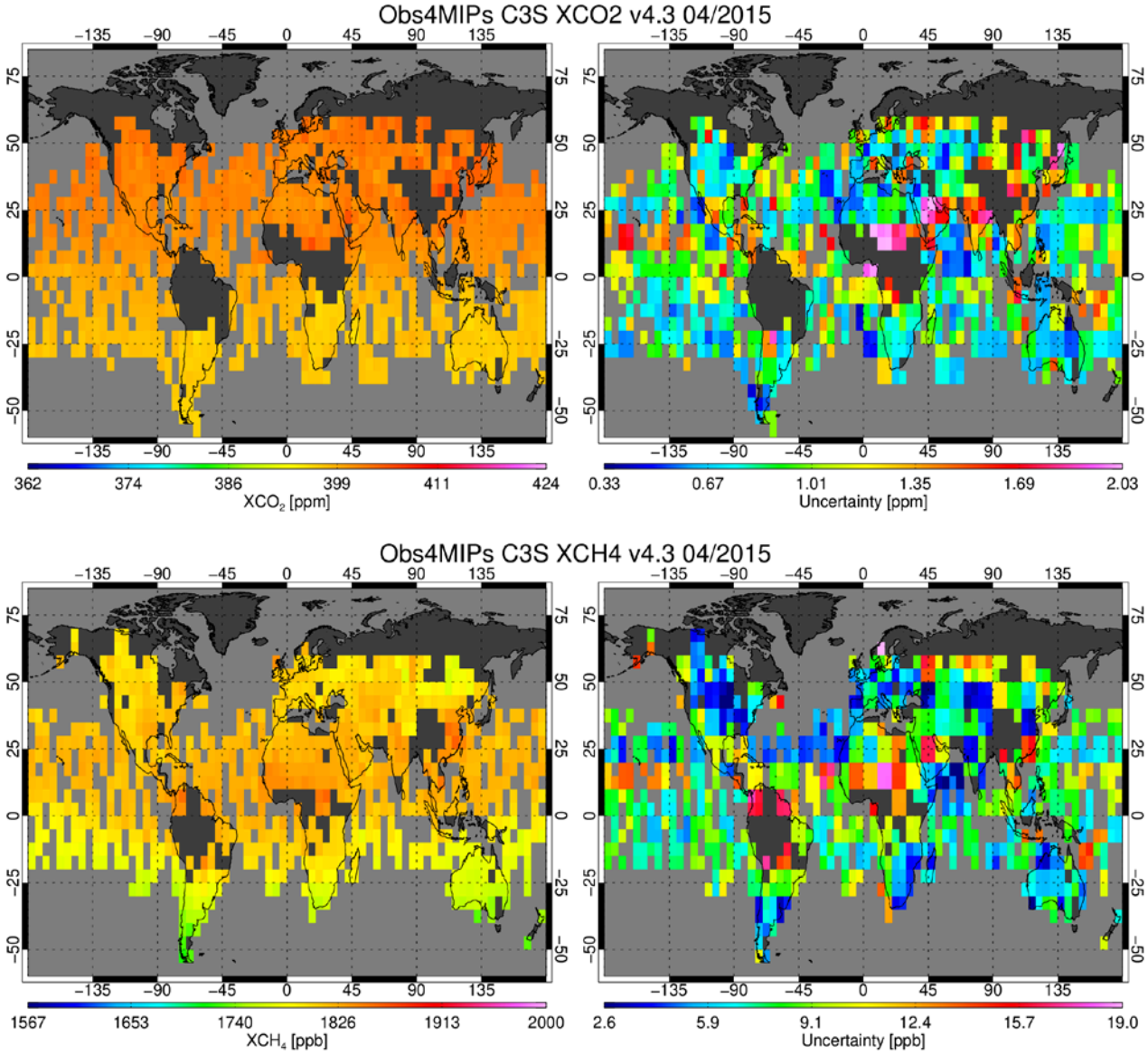

5. References

Araujo and New, 2007: Araujo, M. B. and New, M.: Ensemble forecasting of species distributions, Trends Ecol. Evol., 22, 42–47, doi:10.1016/j.tree.2006.09.010, 2007

Boesch and Anand, 2017: H. Boesch and J. Anand, Algorithm Theoretical Basis Document (ATBD) – ANNEX A for products CO2_GOS_OCFP, CH4_GOS_OCFP & CH4_GOS_OCPR, Copernicus Climate Change Service (C3S) project on satellite-derived Essential Climate Variable (ECV) Greenhouse Gases (CO_2 and CH_4) data products (project C3S_312a_Lot6), Version 1 (21/08/2017), 2017

Bovensmann et al., 1999: Bovensmann, H., Burrows, J. P., Buchwitz, M., Frerick, J., Noel, S., Rozanov, V. V., Chance, K. V., and Goede, A.: SCIAMACHY –Mission Objectives and Measurement Modes, J. Atmos. Sci., 56, 127–150, 1999

Bril et al., 2012: Bril, A.; Oshchepkov, S.; Yokota, T. Application of a probability density function-based atmospheric light-scattering correction to carbon dioxide retrievals from GOSAT over-sea observations. Remote Sensing of the Environment 2012, 117, 301–306

Burrows et al., 1995: Burrows, J. P., Hölzle, E., Goede, A. P. H., Visser, H., and Fricke, W.: SCIAMACHY – Scanning Imaging Absorption Spectrometer for Atmospheric Chartography, Acta Astronaut., 35, 445–451, 1995

Chevallier et al., 2007: Chevallier, F., Br´eon, F.-M., and Rayner, P. J.: Contribution of the Orbiting Carbon Observatory to the estimation of CO2 sources and sinks: Theoretical study in a variational data assimilation framework, J. Geophys. Res., 112, D09307, doi:10.1029/2006JD007375, 2007

Crisp et al., 2017: Crisp, D.; Pollock, H.R.; Rosenberg, R.; Chapsky, L.; Lee, R.A.M.; Oyafuso, F.A.; Frankenberg, C.; O'Dell, C.W.; Bruegge, C.J.; Doran, G.B.; et al. The on-orbit performance of the Orbiting Carbon Observatory-2 (OCO-2) instrument and its radiometrically calibrated products. Atmos. Meas. Tech. 2017, 10, 59–81

Detmers, 2017a: R. Detmers, Algorithm Theoretical Basis Document (ATBD) – ANNEX B for products CO2_GOS_SRFP & CH4_GOS_SRFP, Copernicus Climate Change Service (C3S) project on satellite-derived Essential Climate Variable (ECV) Greenhouse Gases (CO_2 and CH_4) data products (project C3S_312a_Lot6), Version 1 (21/08/2017), 2017

Detmers, 2017b: R. Detmers, Algorithm Theoretical Basis Document (ATBD) – ANNEX C for product CH4_GOS_SRPR, Copernicus Climate Change Service (C3S) project on satellite-derived Essential Climate Variable (ECV) Greenhouse Gases (CO_2 and CH_4) data products (project C3S_312a_Lot6), Version 1 (21/08/2017), 2017

Hagedorn et al., 2005: Hagedorn, R., Doblas-Reyes, F., and Palmer, T.: The rationale behind the success of multi-model ensembles in seasonal forecasting – I. Basic concept, Tellus A, 57, 219–233, doi:10.1111/j.1600-0870.2005.00103.x, 2005

Houweling et al., 2014: Houweling, S., Breon, F.-M., Aben, I., R¨odenbeck, C., Gloor, M., Heimann, M., and Ciais, P.: Inverse modeling of CO2 sources and sinks using satellite data: a synthetic inter-

comparison of measurement techniques and their performance as a function of space and time, Atmos. Chem. Phys., 4, 523–538, doi:10.5194/acp-4-523-2004, 2004

Jacobson et al., 2020: Jacobson, A. R., Schuldt, K. N., Miller, J. B., Oda, T., Tans, P., Arlyn Andrews, Mund, J., Ott, L., Collatz, G. J., Aalto, T., Afshar, S., Aikin, K., Aoki, S., Apadula, F., Baier, B., Bergamaschi, P., Beyersdorf, A., Biraud, S. C., Bollenbacher, A., Bowling, D., Brailsford, G., Abshire, J. B., Chen, G., Huilin Chen, Lukasz Chmura, Sites Climadat, Colomb, A., Conil, S., Cox, A., Cristofanelli, P., Cuevas, E., Curcoll, R., Sloop, C. D., Davis, K., Wekker, S. D., Delmotte, M., DiGangi, J. P., Dlugokencky, E., Ehleringer, J., Elkins, J. W., Emmenegger, L., Fischer, M. L., Forster, G., Frumau, A., Galkowski, M., Gatti, L. V., Gloor, E., Griffis, T., Hammer, S., Haszpra, L., Hatakka, J., Heliasz, M., Hensen, A., Hermanssen, O., Hintsa, E., Holst, J., Jaffe, D., Karion, A., Kawa, S. R., Keeling, R., Keronen, P., Kolari, P., Kominkova, K., Kort, E., Krummel, P., Kubistin, D., Labuschagne, C., Langenfelds, R., Laurent, O., Laurila, T., Lauvaux, T., Law, B., Lee, J., Lehner, I., Leuenberger, M., Levin, I., Levula, J., Lin, J., Lindauer, M., Loh, Z., Lopez, M., Myhre, C. L., Machida, T., Mammarella, I., Manca, G., Manning, A., Manning, A., Marek, M. V., Marklund, P., Martin, M. Y., Matsueda, H., McKain, K., Meijer, H., Meinhardt, F., Miles, N., Miller, C. E., Mölder, M., Montzka, S., Moore, F., Josep-Anton Morgui, Morimoto, S., Munger, B., Jaroslaw Necki, Newman, S., Nichol, S., Niwa, Y., O'Doherty, S., Mikaell Ottosson-Löfvenius, Paplawsky, B., Peischl, J., Peltola, O., Jean-Marc Pichon, Piper, S., Plass-Dölmer, C., Ramonet, M., Reyes-Sanchez, E., Richardson, S., Riris, H., Ryerson, T., Saito, K., Sargent, M., Sasakawa, M., Sawa, Y., Say, D., Scheeren, B., Schmidt, M., Schmidt, A., Schumacher, M., Shepson, P., Shook, M., Stanley, K., Steinbacher, M., Stephens, B., Sweeney, C., Thoning, K., Torn, M., Turnbull, J., Tørseth, K., Bulk, P. V. D., Laan-Luijkx, I. T. V. D., Dinther, D. V., Vermeulen, A., Viner, B., Vitkova, G., Walker, S., Weyrauch, D., Wofsy, S., Worthy, D., Dickon Young, and Miroslaw Zimnoch: CarbonTracker CT2019, https://doi.org/10.25925/39M3-6069, https://www.esrl.noaa.gov/gmd/ccgg/carbontracker/CT2019/, 2020

Karion et al., 2010: Karion, A., Sweeney, C., Tans, P., and Newberger, T.: AirCore: An Innovative Atmospheric Sampling System, J. Atmos. Ocean. Tech., 27, 1839–1853, doi:10.1175/2010JTECHA1448.1, 2010

Kiel et al., 2019: Kiel, M., O'Dell, C. W., Fisher, B., Eldering, A., Nassar, R., MacDonald, C. G., and Wennberg, P. O.: How bias correction goes wrong: measurement of XCO_2 affected by erroneous surface pressure estimates, Atmos. Meas. Tech., 12, 2241–2259, https://doi.org/10.5194/amt-12-2241-2019, 2019

Miller et al., 2007: Miller, C. E., Crisp, D., DeCola, P. L., Olsen, S. C., Randerson, J. T., Michalak, A. M., Alkhaled, A., Rayner, P., Jacob, D. J., Suntharalingam, P., Jones, D. B. A., Denning, A. S., Nicholls, M. E., Doney, S. C., Pawson, S., B¨osch, H., Connor, B. J., Fung, I. Y., O'Brien, D., Salawitch, R. J., Sander, S. P., Sen, B., Tans, P., Toon, G. C., Wennberg, P. O., Wofsy, S. C., Yung, Y. L., and Law, R. M.: Precision requirements for space-based XCO2 data, J. Geophys. Res., 112, D10314, doi:10.1029/2006JD007659, 2007

Noël et al., 2020: XCO2 retrieval for GOSAT and GOSAT-2 based on the FOCAL algorithm, 2020 (in preparation)

O'Dell et al., 2012: O'Dell, C. W., Connor, B., Bösch, H., O'Brien, D., Frankenberg, C., Castano, R., Christi, M., Eldering, D., Fisher, B., Gunson, M., McDuffie, J., Miller, C. E., Natraj, V., Oyafuso, F., Polonsky, I., Smyth, M., Taylor, T., Toon, G. C.,Wennberg, P. O., andWunch, D.: The ACOS CO2 retrieval algorithm – Part 1: Description and validation against synthetic observations, Atmos. Meas. Tech., 5, 99–121, doi:10.5194/amt-5-99-2012, 2012

Rayner and O'Brien, 2001: Rayner, P. J. and O'Brien, D. M.: The utility of remotely sensed CO2 concentration data in surface inversions, Geophys. Res. Lett., 28, 175–178, 2001

Reuter et al., 2011: M. Reuter, H. Bovensmann, M. Buchwitz, J. P. Burrows, B. J. Connor, N. M. Deutscher, D. W. T. Griffith, J. Heymann, G. Keppel-Aleks, J. Messerschmidt, J. Notholt, C. Petri, J. Robinson, O. Schneising, V. Sherlock, V. Velazco, T. Warneke, P. O. Wennberg, D. Wunch: Retrieval of atmospheric CO2 with enhanced accuracy and precision from SCIAMACHY: Validation with FTS measurements and comparison with model results. Journal of Geophysical Research - Atmospheres, 116, D04301, doi: 10.1029/2010JD015047, 2011

Reuter et al., 2012: M. Reuter, M. Buchwitz, O. Schneising, F. Hase, J. Heymann, S. Guerlet, A. J. Cogan, H. Bovensmann, J. P. Burrows: A simple empirical model estimating atmospheric CO2 background concentrations. Atmospheric Measurement Techniques, doi:10.5194/amt-5-1349-2012, 5, 1349-1357, 2012

Reuter et al., 2013: M. Reuter, H. Bösch, H. Bovensmann, A. Bril, M. Buchwitz, A. Butz, J. P. Burrows, C. W. O'Dell, S. Guerlet, O. Hasekamp, J. Heymann, N. Kikuchi, S. Oshchepkov, R. Parker, S. Pfeifer, O. Schneising, T. Yokota, and Y. Yoshida: A joint effort to deliver satellite retrieved atmospheric CO_2 concentrations for surface flux inversions: the ensemble median algorithm EMMA. Atmospheric Chemistry and Physics, doi:10.5194/acp-13-1771-2013, 13, 1771-1780, 2013

Reuter et al., 2016: M. Reuter, H. Bovensmann, M. Buchwitz, J. P. Burrows, J. Heymann, O. Schneising, Algorithm Theoretical Basis Document Version 5 (ATBDv5) - The Bremen Optimal Estimation DOAS (BESD) algorithm for the retrieval of XCO_2, ESA Climate Change Initiative (CCI) for the Essential Climate Variable (ECV) Greenhouse Gases (GHG), Version 5, 2016

Reuter et al., 2017a: M.Reuter, M.Buchwitz, O.Schneising, S.Noël, V.Rozanov, H.Bovensmann and J.P.Burrows: A Fast Atmospheric Trace Gas Retrieval for Hyperspectral Instruments Approximating Multiple Scattering - Part 1: Radiative Transfer and a Potential OCO-2 XCO_2 Retrieval Setup, Remote Sensing, 9(11), 1159; doi:10.3390/rs9111159, 2017

Reuter et al., 2017b: M.Reuter, M.Buchwitz, O.Schneising, S.Noël, H.Bovensmann and J.P.Burrows: A Fast Atmospheric Trace Gas Retrieval for Hyperspectral Instruments Approximating Multiple Scattering - Part 2: Application to XCO_2 Retrievals from OCO-2, Remote Sensing, 9(11), 1102; doi:10.3390/rs9111102, 2017

Reuter et al., 2020: M. Reuter, M. Buchwitz, O. Schneising, S. Noël, H. Bovensmann, J.P. Burrows, H. Boesch, A. Di Noia, J. Anand, R.J. Parker, P. Somkuti, L. Wu, O.P. Hasekamp, I. Aben, A. Kuze, H. Suto, K. Shiomi, Y. Yoshida, I. Morino, D. Crisp, C.W. O'Dell, J. Notholt, C. Petri, T. Warneke, V.A. Velazco, N.M. Deutscher, D.W.T. Griffith, R. Kivi, D.F. Pollard, F. Hase, R. Sussmann, Y.V. Té, K. Strong, S. Roche, M.K. Sha, M. De Mazière, D.G. Feist, L.T. Iraci, C.M. Roehl, C. Retscher, and D. Schepers:

Ensemble-based satellite-derived carbon dioxide and methane column-averaged dry-air mole fraction data sets (2003-2018) for carbon and climate applications, Atmos. Meas. Tech., https://www.atmos-meas-tech.net/13/789/2020, 2020

Rötter et al., 2011: Rötter, R. P., Carter, T. R., Olesen, J. E., and Porter, J. R.: Cropclimate models need an overhaul, Nat. Clim. Change, 1, 175–177, 2011

Rodgers 2000: Rodgers, C. D.: Inverse Methods for Atmospheric Sounding: Theory and Practice, World Scientific Publishing, Singapore, 2000

Schneising et al., 2016: GHG-CCI group at IUP Bremen, Algorithm Theoretical Basis Document (ATBD) - SCIAMACHY WFM-DOAS (WFMD) XCO2 and XCH4 for the Essential Climate Variable (ECV) Greenhouse Gases (GHG), ESA Climate Change Initiative (CCI) for the Essential Climate Variable (ECV) Greenhouse Gases (GHG), Version 5, 2016

Schneising et al., 2019: Schneising, O., Buchwitz, M., Reuter, M., Bovensmann, H., Burrows, J. P., Borsdorff, T., Deutscher, N. M., Feist, D. G., Griffith, D. W. T., Hase, F., Hermans, C., Iraci, L. T., Kivi, R., Landgraf, J., Morino, I., Notholt, J., Petri, C., Pollard, D. F., Roche, S., Shiomi, K., Strong, K., Sussmann, R., Velazco, V. A., Warneke, T., and Wunch, D.: A scientific algorithm to simultaneously retrieve carbon monoxide and methane from TROPOMI onboard Sentinel-5 Precursor, Atmos. Meas. Tech. Discuss., https://www.atmos-meas-tech-discuss.net/amt-2019-243/, in review, 2019.

Tebaldi, C. and Knutti, 2007: Tebaldi, C. and Knutti, R.: The use of the multi-model ensemble in probabilistic climate projections, Philos. Trans. R. Soc. A, 365, 2053–2075, doi:10.1098/rsta.2007.2076, 2007

Vautard et al., 2009: Vautard, R., Schaap, M., Bergstrom, R., Bessagnet, B., Brandt, J., Builtjes, P. J. H., Christensen, J. H., Cuvelier, C., Foltescu, V., Graff, A., Kerschbaumer, A., Krol, M., Roberts, P., Rouil, L., Stern, R., Tarrason, L., Thunis, P., Vignati, E., and Wind, P.: Skill and uncertainty of a regional air quality model ensemble, Atmos. Environ., 43, 4822–4832, doi:10.1016/j.atmosenv.2008.09.083, 2009

Wunch et al., 2011: Wunch, D., Toon, G. C., Blavier, J.-F. L., Washenfelder, R. A., Notholt, J., Connor, B. J., Griffith, D. W. T., Sherlock, V., and Wennberg, P. O.: The Total Carbon Column Observing Network (TCCON), Phil. Trans. R. Soc. A, 369, 2087–2112, doi:10.1098/rsta.2010.0240, 2011

Yokota et al., 2004: Yokota, T., Oguma, H., Morino, I., and Inoue, G.: A nadir looking SWIR sensor to monitor CO2 column density for Japanese GOSAT project, Proceedings of the twenty-fourth international symposium on space technology and science, Miyazaki: Japan Society for Aeronautical and Space Sciences and ISTS, 887–889, 2004

Yoshida et al., 2011: Yoshida, Y., Ota, Y., Eguchi, N., Kikuchi, N., Nobuta, K., Tran, H., Morino, I., and Yokota, T.: Retrieval algorithm for CO2 and CH4 column abundances from short-wavelength infrared spectral observations by the Greenhouse gases observing satellite, Atmos. Meas. Tech., 4, 717–734, doi:10.5194/amt-4-717-2011, 2011

Copernicus Climate Change Service

ECMWF - Shinfield Park, Reading RG2 9AX, UK

Contact: info@copernicus-climate.eu

climate.copernicus.eu copernicus.eu ecmwf.int